12-1-2017

Additive manufacturing techniques and their biomedical applications

Yujing Liu
Edith Cowan University

Wei Wang
Edith Cowan University

Laichang Zhang
School of Engineering

10.15212/FMCH.2017.0110
Liu, Y., Wang, W., & Zhang, L. C. (2017). Additive manufacturing techniques and their biomedical applications. *Family Medicine and Community Health*, https://doi.org/10.15212/FMCH.2017.0110

Family Medicine and Community Health
SYSTEMATIC REVIEW

Additive manufacturing techniques and their biomedical applications

Yujing Liu[1], Wei Wang[2], Lai-Chang Zhang[1]

Abstract

Additive manufacturing (AM), also known as three-dimensional (3D) printing, is gaining increasing attention in medical fields, especially in dental and implant areas. Because AM technologies have many advantages in comparison with traditional technologies, such as the ability to manufacture patient-specific complex components, high material utilization, support of tissue growth, and a unique customized service for individual patients, AM is considered to have a large potential market in medical fields. This brief review presents the recent progress of 3D-printed biomedical materials for bone applications, mainly for metallic materials, including multifunctional alloys with high strength and low Young's modulus, shape memory alloys, and their 3D fabrication by AM technologies. It describes the potential of 3D printing techniques in precision medicine and community health.

Keywords: 3D printing; titanium porous implants; mechanical properties; orthopedic surgery

1. School of Engineering, Edith Cowan University, Perth, WA, Australia
2. School of Medical and Health Sciences, Edith Cowan University, Perth, WA, Australia

CORRESPONDING AUTHOR:
Lai-Chang Zhang
School of Engineering, Edith Cowan University, 270 Joondalup Drive, Joondalup, Perth, WA 6027, Australia
Tel.: +61-8-63042322
Fax: +61-8-63045811
E-mail: lczhangimr@gmail.com; l.zhang@ecu.edu.au

Received 2 September 2016;
Accepted 10 October 2016

Introduction

Demand for implants is increasing because of more patients with bone diseases caused by the growing aged population and traffic accidents [1–3]. Therefore it is important to fabricate high-quality patient-specific implants to reduce the risk of repeated surgical procedures and alleviate patients' pain. However, it is reported that conventional bone repairing techniques, such as bone grafts and distraction osteogenesis, are hard to apply [4, 5]. Additive manufacturing (AM) techniques, also known as three-dimensional (3D) printing, are considered as the most cutting-edge manufacturing technologies to manufacture patient-specific implants based on a layer-wise method. These techniques can produce complex shaped implants with a scaffold structure to satisfy a variety of different needs [1, 6–8]. Moreover, AM could produce patient-specific devices with external geometries derived from the patient's computed tomography (CT) or magnetic resonance imaging (MRI) data. A patient-specific implant has the potential to reduce surgery operation time, restore correct joint kinetics, improve implant fixation, and reduce the risk of repeated surgery [6].

Currently, there are several representative AM techniques, including inkjet printing (IJP), fused deposition modeling (FDM), selective laser sintering (SLS), electron beam melting (EBM), selective laser melting (SLM), and ultrafast laser processing. In particular, the mechanism of the FDM technique

is that the raw material is melted and extruded from a nozzle, and then the melting material cools down gradually after extrusion. An inkjet system dispenses droplets of material onto the selected area of a substrate, and the manufacturing process can be performed in a thermal, air-pressure, electromagnetic, or piezoelectric environment. An SLS system is equipped with a laser source to sinter the powder material, which is deposited on the powder bed. Because of insufficient laser energy to melt the powder completely, SLS-produced components normally have a low relative density. SLM and EBM have a similar processing mechanism based on the layer technique [1]. They use a laser of high energy or an electron beam as the heat source to completely melt the powder material. The powder layer thickness in SLM or EBM is usually between 20 and 100 μm. These two techniques are capable of producing nearly full density parts of high quality and with complex geometries.

However, the selection of suitable metallic materials has become more important because AM-produced components need to meet the specific requirements for different bone implants. For example, load-bearing bone sites need material having great performance such as high strength, light weight, good biocompatibility, and great corrosion resistance. Several materials are believed to be suitable for AM in the implant field. Generally, they can be classified into three categories: metals, ceramics, and polymers [9–26]. This article describe the AM technologies most commonly used to produce medical implants, and then outlines the latest 3D printing applications, including their performance *in vivo* and *in vitro*.

Classification of additive manufacturing processes

FDM techniques

FDM techniques, also called extrusion-based rapid prototyping, fabricate the component with the nozzle by extruding the material on the substrate in layers [27–29]. Normally, the materials used in FDM are polymers such as thin thermoplastic filaments. The nozzle can melt the material rapidly and extrude the liquid according to a scan strategy designed by computer. The liquid material solidifies very fast, and it will be the solid-state substrate for the next fresh layer. Thus to ensure that the interlayer has good adhesion ability, the manufacturing temperature should be kept below the melting point of the material [30]. The main limitations of FDM techniques is that the materials are thin thermoplastic filaments and the raw materials will be affected by the high melting temperature of the manufacturing process [31].

IJP techniques

Similarly to other AM techniques, IJP techniques build up the component from thin layers of the 3D model under computer control [32, 33]. During fabrication, an inkjet print head deposits the liquid binding material, and then a thin powder layer is deposited over the completed region. This process is repeated until the component is manufactured completely. Usually, after the manufacturing process is completed, the binder will be burn off under a high-temperature heat treatment [34]. The binder materials for these techniques are some polymer latex and silica colloid, while the powder material can be metallic, ceramic, and composite powder.

Selective laser sintering

SLS is a kind of AM technique with a layer-wise mechanism [35–37]. The powder is spread on the substrate plate and subsequently sintered by a laser spot. The scanning is controlled by a computer. The powder in a selected area on the powder bed is bound together to build a complete part. Once the component is finished, the loose powder can be collected from the chamber and recycled for future fabrication. Compared with other AM techniques, SLS can use a lager range of material, including polymers, metals, and composites.

Selective laser melting

SLM is an AM technique that can produce the nearly full density part with use of a high-energy source. Similarly to SLS, SLM is a layer-wise technique that manufactures components based on a 3D CAD model under the control of a computer [33, 38–43]. Differently, SLM systems use a laser spot as the input energy to completely melt the powder material; the computer controls the laser beam through a mirror deflection system and then makes the laser beam focus on the powder bed. The input energy of the laser can be up to several kilowatts [44]. The processing chamber is filled with a protective atmosphere (usually argon) during the manufacturing process to prevent the components from being oxidized [6]. A large range of materials, including metals, polymers, and

ceramics [40, 45–50], have been used for production of components. Compared with the components made by traditional technologies, the SLM as-produced counterparts in the forms of the solid and complex scaffold exhibit comparable or even better mechanical properties without any further postprocessing, such as heat treatment [8, 51–54].

Electron beam melting

In principle, EBM techniques have a processing mechanism similar to that of the aforementioned SLM techniques. Both can produce the nearly full density parts; differently, EBM uses an electron beam spot as the source to melt the powder [55, 56]. The building chamber is evacuated to create a vacuum before the component is manufactured. For EBM systems, the powder layer thickness is usually between 20 and 100 μm [57], which is also similar to that for SLM. Before manufacture, the substrate plate needs to be heated to 700°C by the electron beam to decrease residual stresses between the plate and the as-produced component. Also, this can help sinter powder completely to avoid powder smoking [57, 58]. Extensive endeavors have been made to study the processing, microstructure, and performance of EBM as-produced specimens, and most have mainly focused on metals [1, 8, 54, 58, 59]. Meanwhile, many biomedical applications, including knee, hip joint, and jaw replacements, are being fabricated through EBM techniques [60–62].

Ultrafast laser processing

Techniques using ultrafast lasers (picosecond and femtosecond lasers) have been applied for both AM and subtractive manufacturing in ultrahigh precision for true 3D manufacturing [63–67]. The ultrafast lasers with a pulse width of tens of femtoseconds to picoseconds are focused on the selected regions, where the ultrashort pulse reduces heat diffusion to surrounding regions, thereby creating an ultrahigh precision melting pool. Currently, ultrafast lasers are used extensively for fundamental science research and in industry [68]. The applicable materials usually include proteins, polymers, glasses, and metals, even live cells. The ultrafast laser processing products can be used in medical applications such as functional medical stents and in laser-assisted *in situ* keratomileusis based on the unique ultrahigh molecular weight proteins.

Developments in AM for clinical applications

Patient-personalized implants have been proposed and developed with the development of 3D printing techniques recently. Patient-specific implants can be designed and manufactured according to their medical 3D model, such as 3D CT data and MRI data. On one hand, before bone healing surgery is performed, the 3D printing technique can manufacture a 3D facture model of the bone, which could help preoperative planning in terms of analyzing, diagnosing, and designing the individual operation plan for the patient. On the other hand, 3D printing techniques are capable of manufacturing real components, including the screw placements and the customized implants for a specific patient (Table 1) [69]. They can shorten the surgical time and improve the success of the surgery, which are also the main functions and advantages of 3D printing. Previous literature has reported that 3D-printed components have a positive effect on promoting tissue regeneration in *in vitro* and *in vivo* experiments [4, 50, 69, 75].

Preoperative planning for patient-specific implants

Usually, increasing the time in surgery means an increase in the risk of the operation [76]. Therefore researchers have been searching for methods that could reduce the surgery operation time. Fortunately, 3D printing, as an emerging technique, makes it possible to reduce the operation time. It is an accurate method to manufacture the model of the fractured bone for a specific patient. A large number of studies have demonstrated that 3D as-printed models could improve the success of orthopedic surgery [77, 78]. The 3D data of the fractured bone can be derived from CT or MRI examinations of the patient. The real patient-specific 3D model is then produced by 3D printing techniques. The surgery strategy, including the position and size of the operative incision as well as the length and position of the screw insertion, can be determined from the accurate data on the fractured bone for a specific patient.

You et al. [79] reported that 3D printing technology shows great clinical feasibility for treatment of proximal humeral fractures in aged people. With the help of a 3D-printed proximal humeral fracture model, the morphology and structure of the fractured bone could be shown accurately, which was very necessary for determination of the situation related to the classification and the magnitude for the fractured bone

Table 1. Summary of additive manufacturing processing methods and their medical applications

Additive manufacturing technique	Materials	Targeted clinical cases	Comments	References
FDM	Polyether ether ketone	Facial implant	Three-dimensionally printed implants were suitable for the complex bone structure	[70]
FDM	Heterogeneous hydrogel	Three-dimensional heterogeneous hydrogel model	Promoted the repair of osteochondral defects	[71]
FDM	Ti-6Al-4V	Rat implants	Porosity played an important role in tissue ingrowth	[72]
SLM	Ti-24Nb-4Zr-8Sn	Acetabular cup	The implant has high relative density and good mechanical properties	[6]
EBM	Ti-6Al-4V	Human fetal osteoblasts	Very rough surfaces reduced cell proliferation	[73]
EBM	Ti-6Al-4V	Pig skull	Scaffolds were suitable scaffolds for bone ingrowth	[74]

EBM, electron beam melting; FDM, fused deposition modeling; SLM, selective laser melting.

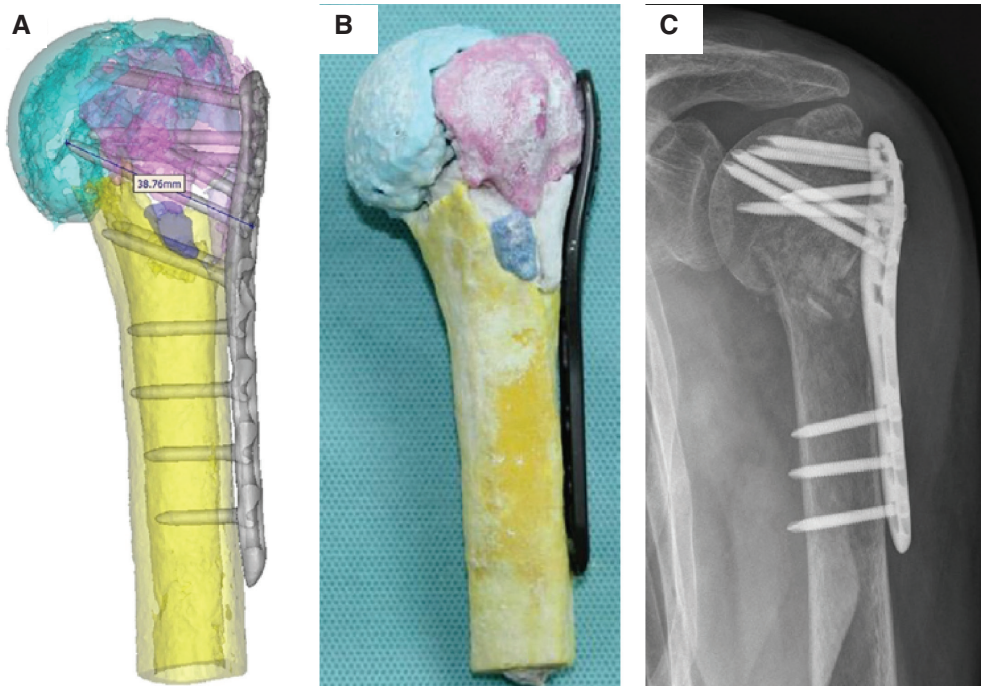

Fig. 1. (A) Three-dimensional shoulder joint simulation data for internal fixation including the design of the length as well as the position of the plate and the screws; (B) three-dimensionally printed model of the simulation of the prepared internal fixation (anterior position); (C) the shoulder joint radiograph after the surgery [79].

(Fig. 1). Thus the treatment strategy can be adjusted and optimized to reduce the intraoperative fracture prior to surgery [79]. Sugawara et al. [80] established a method based on a 3D printing technique to improve the accuracy of pedicle screw insertion, thereby decreasing the surgery time. Three types of 3D templates were produced for determination of the accurate

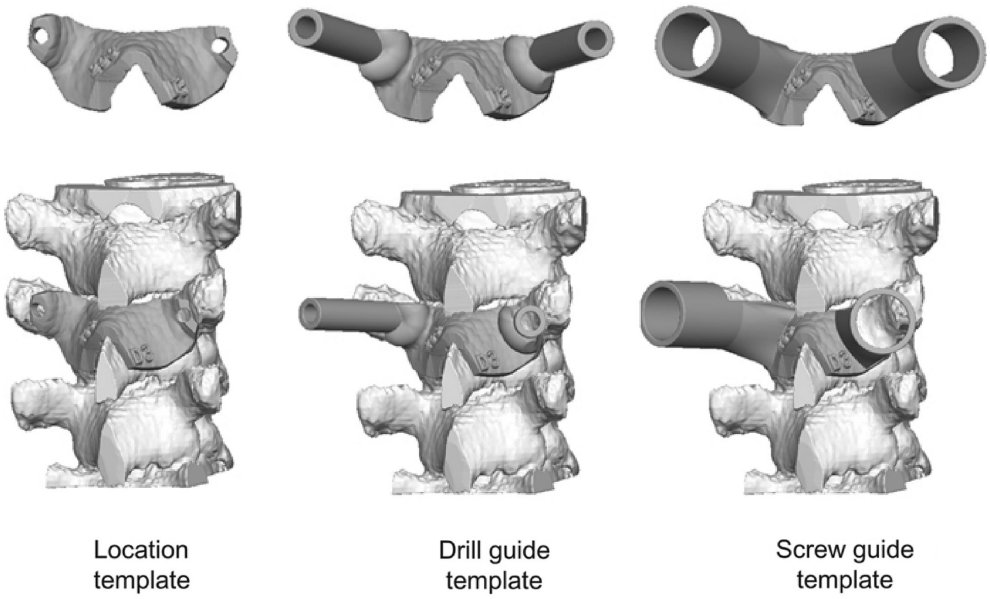

Fig. 2. Three types of templates produced for helping or accurate guidance of the pedicle screw insertion [80].

position of the pedicle screw insertion (Fig. 2). The simulation of the screw insertion was conducted with the templates. Ten patients were selected for surgery, and the results showed that this method can improve the accuracy of screw insertion.

The effect of three-dimensionally printed implants

To produce a high-quality implant, it is necessary to understand in depth the structure of natural bone. It is well known that bone tissue can be divided into two parts (i.e., cancellous and cortical bone). In particular, about 50–90 vol% of cancellous bone is porous. However, the porosity of cortical bone is less than 10 vol% [81]. The target of bone replacement should be a structure similar to that of natural bone so that the implant can promote bone tissue regeneration. The 3D printing techniques have ability to manufacture porous or scaffold structures with a complex patient-specific shape and geometry, variation in the porosity, and a suitable material, which can ensure the implant is similar to natural bone. The porous structure can mimic real bone to improve bio-transport properties inside the implant thereby creating a friendly environment for bone cells ingrowth. Furthermore, such a structure can obtain a high strength and low stiffness (i.e. a low Young's modulus) by manipulating the microstructure therefore the mechanical properties of the implant material used. Titanium and its alloys are metals commonly used for 3D printing techniques. Porous Ti-6Al-4V scaffolds have been studied extensively in terms of processing, mechanical properties, and biocompatibility. Li et al. [58] studied the mechanical properties of rhombic dodecahedron Ti-6Al-4V porous cells (Fig. 3). The results showed a good linear relationship, with a higher exponential factor n of approximately 2.7 compared with the ideal stochastic open cellular foams with a factor of approximately 1.5 (Fig. 3B).

Zhang et al. [6] produced a beta-type Ti-24Nb-4Zr-8Sn biomedical titanium alloy acetabular cup by SLM (Fig. 4). Liu et al. [14] reported an optimized scaffold structure with 85% porosity produced by Ti-24Nb-4Zr-8Sn. The relative density is affected by the laser scanning speed and input energy. The best quality component, with 99.3% relative density, can be achieved with a scan speed of 750 mm/s with a laser power of 175 W. The compression testing results show the strength could reach at 51 MPa with a ductility exceeding 14%. These results illustrate that titanium alloys would be suitable materials for artificial implants. *In vivo* tests showed that a porous titanium alloy scaffold component manufactured by 3D printing techniques could result in fast bone tissue ingrowth [82, 83]. The SLM technique and the EBM technique can both produce components with nearly full density, so researchers are investigating the differences between these two

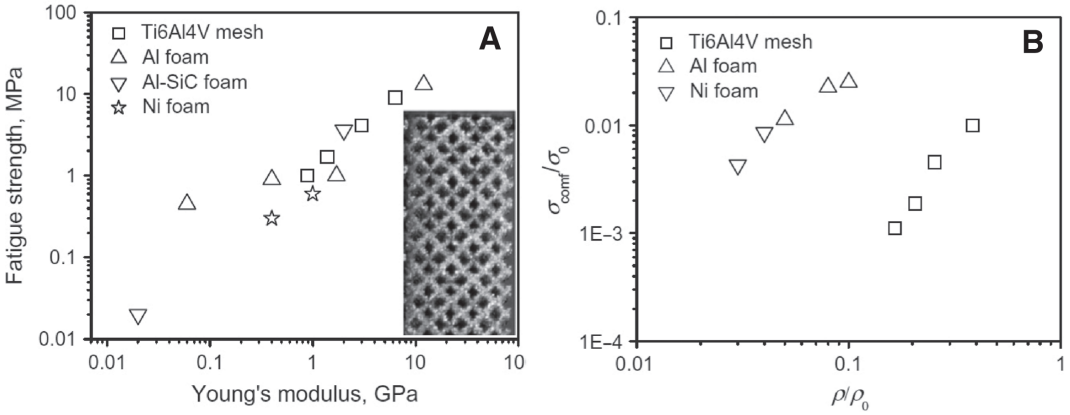

Fig. 3. Mechanical properties of rhombic dodecahedron Ti-6Al-4V porous cells: (A) the relationship between the fatigue strength and the Young's modulus; (B) the relationship between the fatigue strength and the relative density [58].

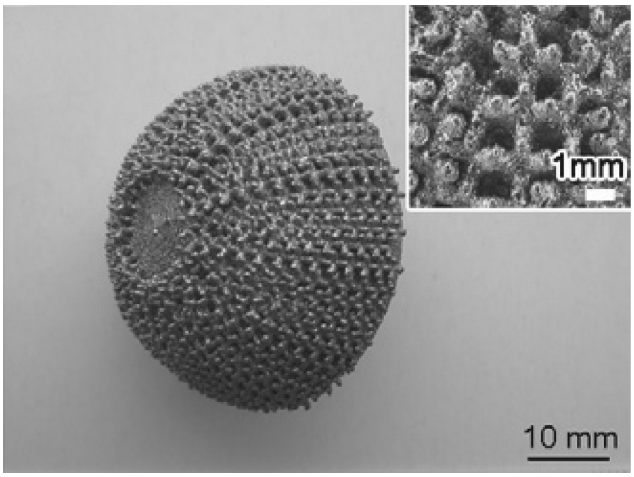

Fig. 4. An acetabular cup made of Ti-24Nb-4Zr-8Sn alloy manufactured by selective laser melting [6].

techniques. Liu et al. [1] compared these two techniques by testing the mechanical properties of the same titanium alloy porous specimens fabricated by SLM and EBM respectively. They found that the microstructures of these two types of as-produced samples exhibit significant differences resulting from the different processing temperature in the 3D printing process. Besides, the relative density of EBM-produced specimens is higher than that of SLM-produced ones, which limits the influence on compressive testing results (Fig. 5A). The results show that the SLM-produced specimens have a scattered fatigue life owing to big defects inside the strut (Fig. 5B). Moreover, a 3D-printed Ti-24Nb-4Zr-8Sn cage has outstanding osseointegration and better mechanical properties than the traditional polyether ether ketone (PEEK) cage, illustrating excellent potential for clinical implants [82, 83].

Kumar et al. [84] tested cell-derived decellularized extracellular matrix (dECM) for porous Ti-6Al-4V scaffolds *in vitro*. The flow diagram of the decellularization process is shown in Fig. 6. The bioactive factors are found in the extracellular matrix, which may improve the cell functionality growth on Ti-6Al-4V scaffolds.

Some ceramic materials can also be used for 3D-printed implants. Fielding and Bose [85] suggested that 3D-printed calcium phosphate scaffolds can play a significant part in bone replacement applications. They manufactured scaffolds of pure and SiO_2/ZnO-doped tricalcium phosphate and implanted them in a bone defect to observe the effect. The results show that there is strong mechanical interlocking between the implant and its surrounding tissue. The addition of dopants had no effect on the dissolution behaviors *in vivo*.

Here, several examples of 3D-printed implants are described to understand how 3D-printed implants improve the effect of the surgery. To investigate the influence of 3D architecture and structure on tissue regeneration, Fedorovich et al. [72] designed and fabricated a 3D heterogeneous hydrogel model using a 3D fiber deposition technique (Fig. 7). They observed excellent bone tissue formation both *in vitro* and *in vivo* at different locations of the 3D structure (Fig. 7C). It is believed that this technology could promote the repair of osteochondral defects.

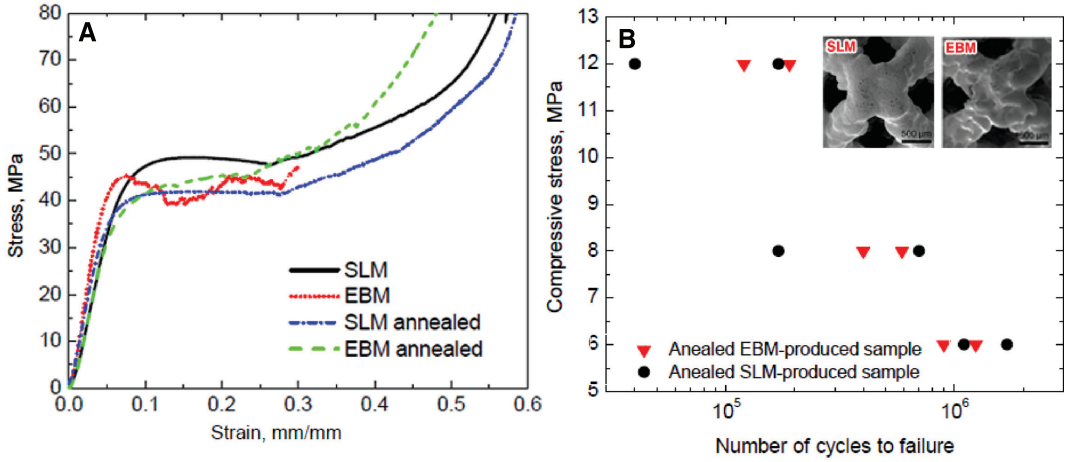

Fig. 5. Comparison of the mechanical properties of Ti-24Nb-4Zr-8Sn alloy components manufactured by selective laser melting (SLM) and electron beam melting (EBM): (A) the compressive strain–stress curves for porous specimens; (B) the fatigue results for the EBM and SLM specimens [1].

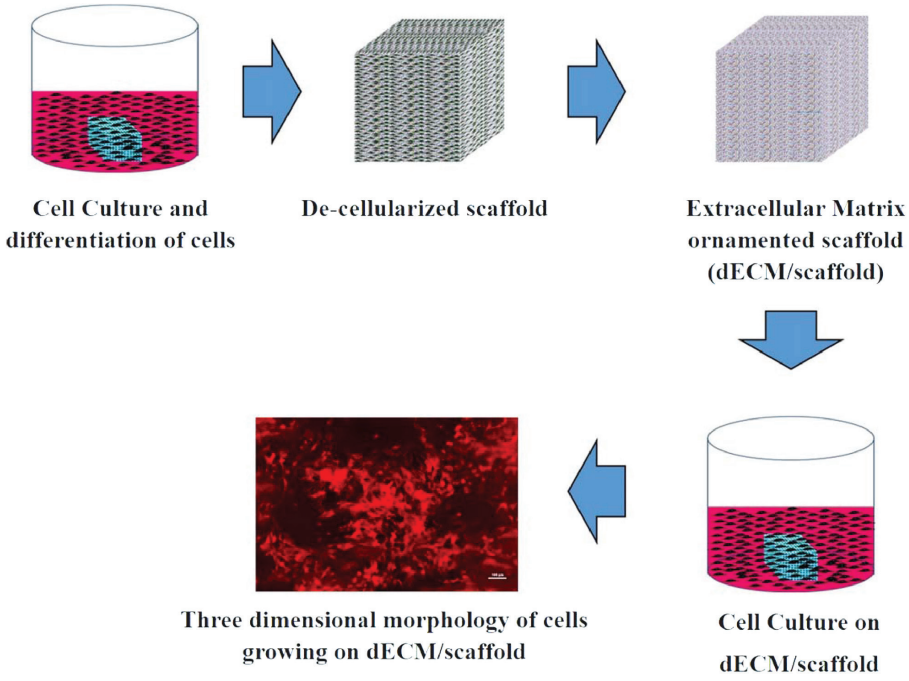

Fig. 6. The flow diagram of the decellularization process for the porous Ti-6Al-4V scaffolds [84].
dECM, decellularized extracellular matrix.

3D-printed implants for specific patients also have great potential to improve the development of orthopedic surgery. Gerbino et al. [71] studied the effect of the facial implant produced by rapid prototyping technology using a PEEK material for more than 10 patients (Fig. 8). The 3D-printed implants were found to be satisfactory in terms of the shape, size, and position, even for the complex bone structure.

Imanishi and Choong [70] reported successful reconstruction with a prosthetic calcaneus based on a 3D printing technique for the first time. They produced a titanium calcaneal implant (Fig. 9A) using an EBM system to reconstruct the

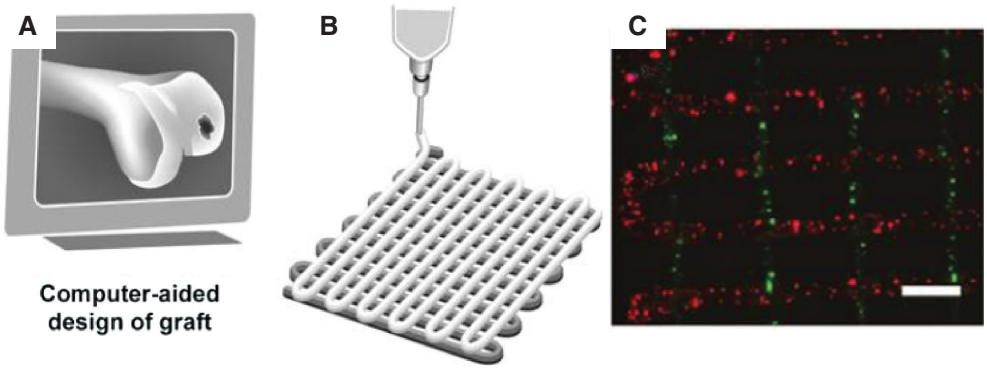

Fig. 7. The process of the fabricated a 3D heterogeneous hydrogel model using 3D fiber deposition technique [72].

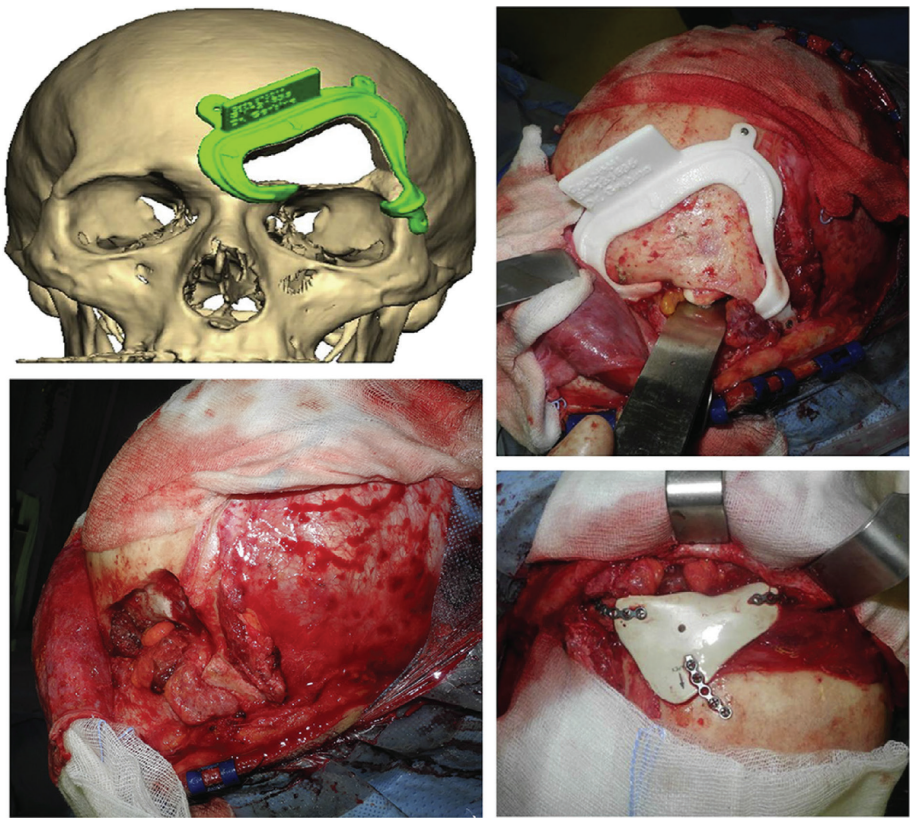

Fig. 8. The process for 3D-printed facial implant surgery [71].

defect by means of total calcanectomy. The EBM-produced calcaneal prosthesis matched well with the talus and cuboid, and the patient could walk on bare feet without any major complications from 5 months after surgery (Figs. 9B and C). The patient-specific titanium calcaneal prosthesis is ready for use within several days from order. The titanium implant is light and has high strength and a complex structure, which are important factors for successful performance of this surgical procedure [70].

Mangano et al. [86] described a method for the design and production of custom implants for a maxillary defect for 10 patients. The patient-specific implants match the defect area

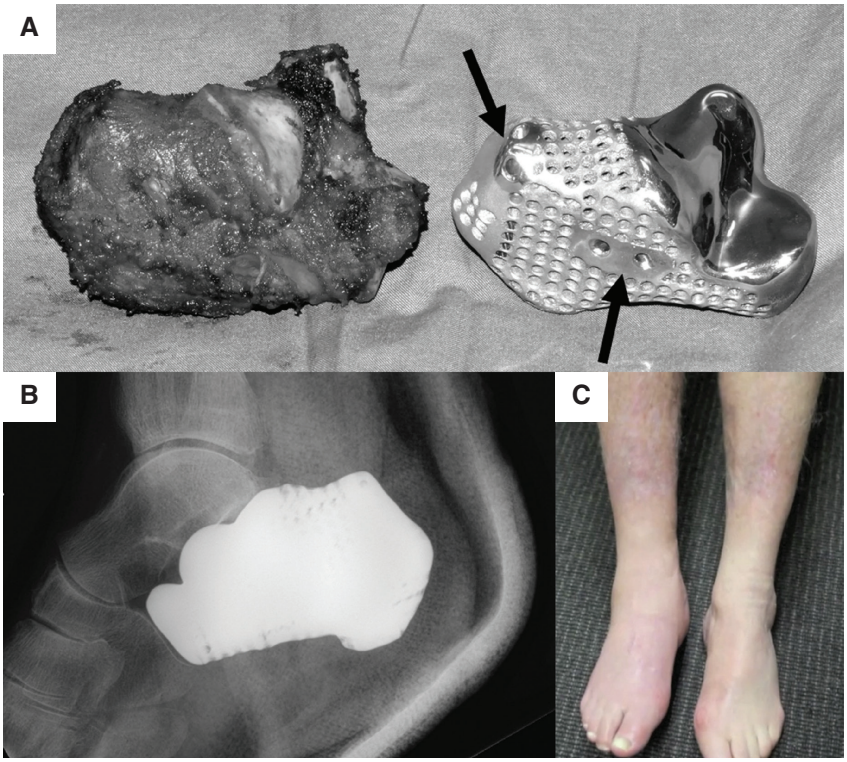

Fig. 9. (A, B) 3D-printed patient-specific titanium calcaneal implant, and (C) patient walking on bare feet at the 5-month follow-up [70].

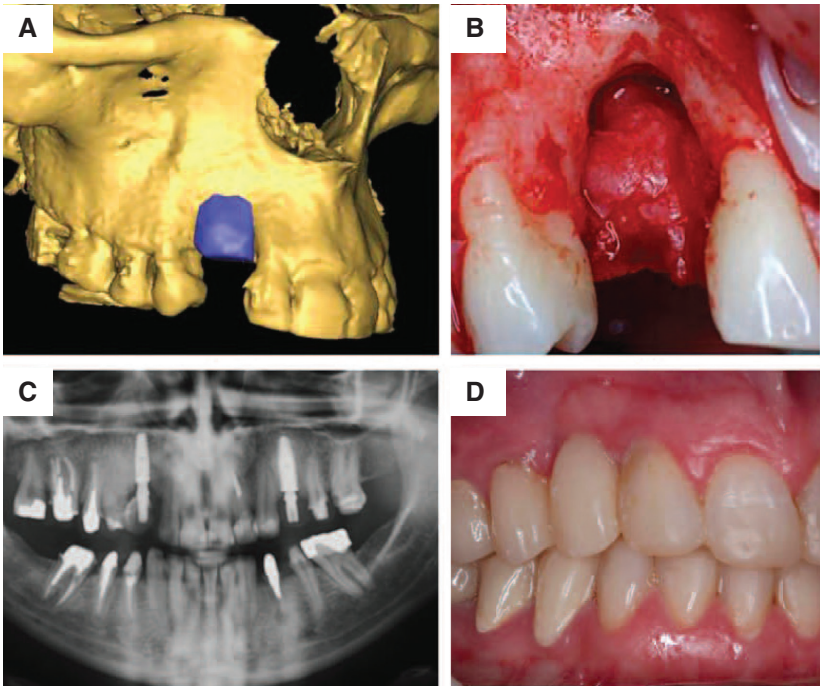

Fig. 10. (A) The 3D data of the maxilla, (B) the morphology of the defect, (C) computed tomography image of the maxilla after surgery, and (D) the maxilla after 1 year, without implant loss [86].

well with satisfactory size and shape (Fig. 10). These implants can be inserted easily, which reduce the surgery time and improves healing.

Conclusion

This brief review has described the recent development of 3D printing techniques using different materials, including metals, ceramics, and polymers, in terms of clinical applications. These techniques can produce implants with multiple complex shapes, porous structures, and made of materials suitable to for use in the medical field. They have been considered as the most promising alternative technologies to help in patient-specific preoperative planning, reduce the surgery operation time, and improve the success rate of implant surgery. Because of on biomaterials, the 3D printing technologies have great potential in precision medicine and community health. Further studies need to focus on improving the mechanical properties of implants manufactured by 3D printing, such as through the development of new biomaterials with better mechanical properties, improving the accuracy of the porous implant, and producing a graded porous structure with an optimized Young's modulus to match the surrounding tissue.

Acknowledgment

This research was supported under the Australian Research Council's Projects funding scheme (DP110101653).

Conflict of interest

The authors declare no conflict of interest.

Funding

This research received no specific grant from any funding agency in the public, commercial, or from non-profit sectors.

References

1. Liu YJ, Li SJ, Wang HL, Hou WT, Hao YL, Yang R, et al. Microstructure, defects and mechanical behavior of beta-type titanium porous structures manufactured by electron beam melting and selective laser melting. Acta Mater 2016;113:56–7.
2. Liu YJ, Zhao X, Zhang LC, Habibi D, Xie Z. Architectural design of diamond-like carbon coatings for long-lasting joint replacements. Mater Sci Eng C 2013;33(5):2788–94.
3. Liu YJ, Wang HL, Li SJ, Wang SG, Wang WJ, Hou WT, et al. Compressive and fatigue behavior of beta-type titanium porous structures fabricated by electron beam melting. Acta Mater 2017;126:58–66.
4. Arealis G, Nikolaou VS. Bone printing: new frontiers in the treatment of bone defects. Injury 2015;46:S20–2.
5. Ronga M, Fagetti A, Canton G, Paiusco E, Surace MF, Cherubino P. Clinical applications of growth factors in bone injuries: experience with BMPs. Injury 2013;44:S34–9.
6. Zhang LC, Klemm D, Eckert J, Hao YL, Sercombe TB. Manufacture by selective laser melting and mechanical behavior of a biomedical Ti–24Nb–4Zr–8Sn alloy. Scr Mater 2011; 65(1):21–4.
7. Zhang LC, Attar H. Selective laser melting of titanium alloys and titanium matrix composites for biomedical applications: a review. Adv Eng Mater 2016;18(4):463–75.
8. Liu YJ, Li SJ, Hou WT, Wang SG, Hao YL, Yang R, et al. Electron beam melted beta-type Ti–24Nb–4Zr–8Sn porous structures with high strength-to-modulus ratio. J Mater Sci Technol 2016;32(6):505–8.
9. Ehtemam-Haghighi S, Liu Y, Cao G, Zhang LC. Phase transition, microstructural evolution and mechanical properties of Ti–Nb–Fe alloys induced by Fe addition. Mater Des 2016;97:279–86.
10. Dai N, Zhang LC, Zhang J, Zhang X, Ni Q, Chen Y, et al. Distinction in corrosion resistance of selective laser melted Ti–6Al–4V alloy on different planes. Corros Sci 2016;111:703–10.
11. Ehtemam-Haghighi S, Liu YJ, Cao G, Zhang LC. Influence of Nb on the β→α″ martensitic phase transformation and properties of the newly designed Ti–Fe–Nb alloys. Mater Sci Eng C 2016;60:503–10.
12. Dai N, Zhang LC, Zhang J, Chen Q, Wu M. Corrosion behaviour of selective laser melted Ti–6Al–4V alloy in NaCl solution. Corros Sci 2016;102:484–9.
13. Zhang LC, Attar H, Calin M, Eckert J. Review on manufacture by selective laser melting and properties of titanium based materials for biomedical applications. Mater Technol Adv Perform Mater 2016;31(2):66–76.
14. Liu YJ, Li XP, Zhang LC, Sercombe TB. Processing and properties of topologically optimised biomedical Ti–24Nb–4Zr–8Sn scaffolds manufactured by selective laser melting. Mater Sci Eng A 2015;642:268–78.
15. Haghighi SE, Lu H, Jian G, Cao G, Habibi D, Zhang LC. Effect of α″ martensite on the microstructure and mechanical properties of beta-type Ti–Fe–Ta alloys. Mater Des 2015;76:47–54.
16. Attar H, Löber L, Funk A, Calin M, Zhang LC, Prashanth K, et al. Mechanical behavior of porous commercially pure Ti and

Ti–TiB composite Materials manufactured by selective laser melting. Mater Sci Eng A 2015;625:350–6.

17. Zhang LC, Lu H-B, Mickel C, Eckert J. Ductile ultrafine-grained Ti-based alloys with high yield strength. Appl Phys Lett 2007;91:051906.
18. Zhang LC, Xu J, Ma E. Mechanically alloyed amorphous $Ti_{50}(Cu_{0.45}Ni_{0.55})_{44-x}Al_xSi_4B_2$ alloys with supercooled liquid region. J Mater Res 2002;17(07):1743–9.
19. Lu H, Poh C, Zhang LC, Guo Z, Yu X, Liu H. Dehydrogenation characteristics of Ti-and Ni/Ti-catalyzed Mg hydrides. J Alloys Compd 2009;481(1):152–5.
20. Zhang LC, Das J, Lu H, Duhamel C, Calin M, Eckert J. High strength Ti–Fe–Sn ultrafine composites with large plasticity. Scr Mater 2007;57(2):101–4.
21. Calin M, Zhang LC, Eckert J. Tailoring of microstructure and mechanical properties of a Ti-based bulk metallic glass-forming alloy. Scr Mater 2007;57(12):1101–4.
22. Attar H, Prashanth K, Chaubey A, Calin M, Zhang LC, Scudino S, et al. Comparison of wear properties of commercially pure titanium prepared by selective laser melting and casting processes. Mater Lett 2015;142:38–41.
23. Zhang LC, Shen Z, Xu J. Glass formation in a (Ti, Zr, Hf)–(Cu, Ni, Ag)–Al high-order alloy system by mechanical alloying. J Mater Res 2003;18(9):2141–9.
24. Zhang LC, Shen Z, Xu J. Mechanically milling-induced amorphization in Sn-containing Ti-based multicomponent alloy systems. Mater Sci Eng A 2005;394(1):204–9.
25. Zhang LC, Xu J. Glass-forming ability of melt-spun multicomponent (Ti, Zr, Hf)–(Cu, Ni, Co)–Al alloys with equiatomic substitution. J Non-cryst Solids 2004;347(1):166–72.
26. Ehtemam-Haghighi S, Prashanth KG, Attar H, Chaubey AK, Cao GH, Zhang LC. Evaluation of mechanical and wear properties of Ti–xNb–7Fe alloys designed for biomedical applications. Mater Des 2016:111:592–9.
27. Skowyra J, Pietrzak K, Alhnan MA. Fabrication of extended-release patient-tailored prednisolone tablets via fused deposition modelling (FDM) 3D printing. Eur J Pharm Sci 2015;68:11–7.
28. Rayegani F, Onwubolu GC. Fused deposition modelling (FDM) process parameter prediction and optimization using group method for data handling (GMDH) and differential evolution (DE). Int J Adv Manuf Technol 2014;73(1–4):509–19.
29. Meakin J, Shepherd D, Hukins D. Fused deposition models from CT scans. Br J Radiol 2014;77(918):504–7.
30. Bártolo PJ, Almeida HA, Rezende RA, Laoui T, Bidanda B. Advanced processes to fabricate scaffolds for tissue engineering. In: Bidanda B, Bártolo PJ, editors. Virtual Prototyping and bio manufacturing in medical applications. New York: Springer; 2008. pp. 149–70.
31. Abdelaal OA, Darwish SM. Review of rapid prototyping techniques for tissue engineering scaffolds fabrication. In: Öchsner A, da Silva LFM, Altenbach H, editors. Characterization and development of biosystems and biomaterials. Berlin: Springer; 2013. pp. 33–54.
32. Chiolerio A, Virga A, Pandolfi P, Martino P, Rivolo P, Geobaldo F, et al. Direct patterning of silver particles on porous silicon by inkjet printing of a silver salt via in-situ reduction. Nanoscale Res Lett 2012;7(1):1.
33. Liu X, Shen Y, Yang R, Zou S, Ji X, Shi L, et al. Inkjet printing assisted synthesis of multicomponent mesoporous metal oxides for ultrafast catalyst exploration. Nano Lett 2012;12(11):5733–9.
34. Woesz A. Rapid prototyping to produce porous scaffolds with controlled architecture for possible use in bone tissue engineering. In: Bidanda B, Bártolo PJ, editors. Virtual prototyping and bio manufacturing in medical applications. New York: Springer; 2008. pp. 171–206.
35. Olakanmi E, Cochrane R, Dalgarno K. A review on selective laser sintering/melting (SLS/SLM) of aluminium alloy powders: processing, microstructure, and properties. Prog Mater Sci 2015;74:401–77.
36. Mazzoli A. Selective laser sintering in biomedical engineering. Med Biol Eng Comput 2013;51(3):245–56.
37. Olakanmi E. Selective laser sintering/melting (SLS/SLM) of pure Al, Al–Mg, and Al–Si powders: effect of processing conditions and powder properties. J Mater Process Technol 2013;213(8):1387–405.
38. Kruth J-P, Mercelis P, Van Vaerenbergh J, Froyen L, Rombouts M. Binding mechanisms in selective laser sintering and selective laser melting. Rapid Prototyp J 2005;11(1):26–36.
39. Attar H, Calin M, Zhang LC, Scudino S, Eckert J. Manufacture by selective laser melting and mechanical behavior of commercially pure titanium. Mater Sci Eng A 2014;593:170–7.
40. Attar H, Bönisch M, Calin M, Zhang LC, Scudino S, Eckert J. Selective laser melting of in situ titanium–titanium boride composites: processing, microstructure and mechanical properties. Acta Mater 2014;76(9):13–22.
41. Wang X, Zhang LC, Fang M, Sercombe TB. The effect of atmosphere on the structure and properties of a selective laser melted Al–12Si alloy. Mater Sci Eng A 2014;597:370–5.
42. Li X, Wang X, Saunders M, Suvorova A, Zhang LC, Liu Y, et al. A selective laser melting and solution heat treatment refined Al–12Si alloy with a controllable ultrafine eutectic microstructure and 25% tensile ductility. Acta Mater 2015;95:74–82.

43. Chen Y, Zhang J, Dai N, Qin P, Attar H, Zhang LC. Corrosion behaviour of selective laser melted Ti-TiB biocomposite in simulated body fluid. Electrochim Acta 2017;232:89–97.
44. Chua CK, Leong KF. 3D printing and additive manufacturing: principles and applications. London: World Scientific Publishing Co Inc.; 2015.
45. Liu ZH, Zhang DQ, Chua CK, Leong KF. Crystal structure analysis of M2 high speed steel parts produced by selective laser melting. Mater Charact 2013;84(10):72–80.
46. Ramirez DA, Murr LE, Martinez E, Hernandez DH, Martinez JL, Machado BI, et al. Novel precipitate-microstructural architecture developed in the fabrication of solid copper components by additive manufacturing using electron beam melting. Acta Mater 2011;59(10):4088–99.
47. Sun SH, Koizumi Y, Kurosu S, Li YP, Chiba A. Phase and grain size inhomogeneity and their influences on creep behavior of Co–Cr–Mo alloy additive manufactured by electron beam melting. Acta Mater 2015;86:305–18.
48. Gu D, Hagedorn YC, Meiners W, Meng G, Rui JS, Wissenbach K, et al. Densification behavior, microstructure evolution, and wear performance of selective laser melting processed commercially pure titanium. Acta Mater 2012;60(9):3849–60.
49. Riedlbauer D, Drexler M, Drummer D, Steinmann P, Mergheim J. Modelling, simulation and experimental validation of heat transfer in selective laser melting of the polymeric material PA12. Comput Mater Sci 2014;93:239–48.
50. Wilkes J, Hagedorn Y-C, Meiners W, Wissenbach K. Additive manufacturing of ZrO_2–Al_2O_3 ceramic components by selective laser melting. Rapid Prototyp J 2013;19(1):51–7.
51. Prashanth K, Scudino S, Klauss H, Surreddi KB, Löber L, Wang Z, et al. Microstructure and mechanical properties of Al–12Si produced by selective laser melting: effect of heat treatment. Mater Sci Eng A 2014;590:153–60.
52. Thijs L, Verhaeghe F, Craeghs T, Humbeeck JV, Kruth JP. A study of the microstructural evolution during selective laser melting of Ti–6Al–4V. Acta Mater 2010;58(9):3303–12.
53. Hrabe NW, Heinl P, Flinn B, Körner C, Bordia RK. Compression-compression fatigue of selective electron beam melted cellular titanium (Ti-6Al-4V). J Biomed Mater Res Part B Appl Biomater 2011;99(2):313–20.
54. Zhao S, Li S, Hou W, Hao Y, Yang R, Misra R. The influence of cell morphology on the compressive fatigue behavior of Ti-6Al-4V meshes fabricated by electron beam melting. J Mech Behav Biomed Mater 2016;59:251–64.
55. Murr LE, Gaytan SM, Ramirez DA, Martinez E, Hernandez J, Amato KN, et al. Metal fabrication by additive manufacturing using laser and electron beam melting technologies. J Mater Sci Technol 2012;28(1):1–14.
56. Hrabe N, Quinn T. Effects of processing on microstructure and mechanical properties of a titanium alloy (Ti–6Al–4V) fabricated using electron beam melting (EBM), part 2: energy input, orientation, and location. Mater Sci Eng A 2013;573:271–7.
57. Sing SL, An J, Yeong WY, Wiria FE. Laser and electron-beam powder-bed additive manufacturing of metallic implants: a review on processes, materials and designs. J Orthop Res 2015;34(3):369–85.
58. Li S, Murr L, Cheng X, Zhang Z, Hao Y, Yang R, et al. Compression fatigue behavior of Ti–6Al–4V mesh arrays fabricated by electron beam melting. Acta Mater 2012;60(3):793–802.
59. Li S, Xu Q, Wang Z, Hou W, Hao Y, Yang R, et al. Influence of cell shape on mechanical properties of Ti–6Al–4V meshes fabricated by electron beam melting method. Acta Biomater 2014;10(10):4537–47.
60. Cronskär M, Bäckström M, Rännar L-E. Production of customized hip stem prostheses-a comparison between conventional machining and electron beam melting (EBM). Rapid Prototyp J 2013;19(5):365–72.
61. Mazzoli A, Germani M, Raffaeli R. Direct fabrication through electron beam melting technology of custom cranial implants designed in a PHANToM-based haptic environment. Mater Des 2009;30(8):3186–92.
62. Jardini AL, Larosa MA, Maciel Filho R, de Carvalho Zavaglia CA, Bernardes LF, Lambert CS, et al. Cranial reconstruction: 3D biomodel and custom-built implant created using additive manufacturing. J Cranio-Maxillofac Surg 2014;42(8):1877–84.
63. Yong DS, Li YC, Chang NS, Campagnola PJ, Chen SJ. Fabrication of three-dimensional multi-protein microstructures for cell migration and adhesion enhancement. Biomed Opt Express 2015;6(2):480–90.
64. Ovsianikov A, Gruene M, Pflaum M, Koch L, Maiorana F, Wilhelmi M, et al. Laser printing of cells into 3D scaffolds. Biofabrication 2010;2(1):65–117.
65. Mačiulaitis J, Deveikytė M, Rekštytė S, Bratchikov M, Darinskas A, Šimbelytė A, et al. Preclinical study of SZ2080 material 3D microstructured scaffolds for cartilage tissue engineering made by femtosecond direct laser writing lithography. Biofabrication 2015;7(1):015015.
66. Kufelt O, Eltamer A, Sehring C, Schliewolter S, Chichkov BN. Hyaluronic acid based materials for scaffolding via two-photon polymerization. Biomacromolecules 2014;15(2):650–9.

67. Malinauskas M, Rekštytė S, Lukoševičius L, Butkus S, Balčiūnas E, Pečiukaitytė M, et al. 3D microporous scaffolds manufactured via combination of fused filament fabrication and direct laser writing ablation. Micromachines 2014;5(4):839–58.
68. Sugioka K. Progress in ultrafast laser processing and future prospects. Nanophotonics 2016;5:17–37.
69. Mok S-W, Nizak R, Fu S-C, Ho K-WK, Qin L, Saris DB, et al. From the printer: potential of three-dimensional printing for orthopaedic applications. J Orthop Translat 2016;6:42–9.
70. Gerbino G, Zavattero E, Zenga F, Bianchi FA, Garzino-Demo P, Berrone S. Primary and secondary reconstruction of complex craniofacial defects using polyetheretherketone custom-made implants. J Cranio-Maxillofac Surg 2015;43(8):1356–63.
71. Fedorovich NE, Schuurman W, Wijnberg HM, Prins H-J, van Weeren PR, Malda J, et al. Biofabrication of osteochondral tissue equivalents by printing topologically defined, cell-laden hydrogel scaffolds. Tissue Eng Part C Methods 2011;18(1):33–44.
72. Bandyopadhyay A, Espana F, Balla VK, Bose S, Ohgami Y, Davies NM. Influence of porosity on mechanical properties and in vivo response of Ti6Al4V implants. Acta Biomater 2010;6(4):1640–8.
73. Ponader S, Vairaktaris E, Heinl P, Wilmowsky CV, Rottmair A, Körner C, et al. Effects of topographical surface modifications of electron beam melted Ti-6Al-4V titanium on human fetal osteoblasts. J Biomed Mater Res A 2008;84(4):1111–9.
74. Ponader S, Von Wilmowsky C, Widenmayer M, Lutz R, Heinl P, Körner C, et al. In vivo performance of selective electron beam-melted Ti-6Al-4V structures. J Biomed Mater Res A 2010;92A(1):56–62.
75. Imanishi J, Choong PF. Three-dimensional printed calcaneal prosthesis following total calcanectomy. Int J Surg Case Rep 2015;10:83–7.
76. Naranje S, Lendway L, Mehle S, Gioe TJ. Does operative time affect infection rate in primary total knee arthroplasty? Clin Orthop Relat Res 2015;473(1):64–9.
77. Ansari M, Yao Q, Gu Q, Wei B, Liu S, Zhang X, et al. Advantages of 3D printed hip model over conventional imaging methods. Sci Lett 2015;3(2):98–101.
78. O'Brien EK, Wayne DB, Barsness KA, McGaghie WC, Barsuk JH. Use of 3D printing for medical education models in transplantation medicine: a critical review. Curr Transplant Rep 2016;3(1):109–19.
79. You W, Liu L, Chen H, Xiong J, Wang D, Huang J, et al. Application of 3D printing technology on the treatment of complex proximal humeral fractures (Neer3-part and 4-part) in old people. Orthop Traumatol Surg Res 2016;102(7):897–903.
80. Sugawara T, Higashiyama N, Kaneyama S, Takabatake M, Watanabe N, Uchida F, et al. Multistep pedicle screw insertion procedure with patient-specific lamina fit-and-lock templates for the thoracic spine: clinical article. J Neurosurg Spine 2013;19(2):185–90.
81. Bose S, Vahabzadeh S, Bandyopadhyay A. Bone tissue engineering using 3D printing. Mater Today 2013;16(12):496–504.
82. Wu SH, Li Y, Zhang YQ, Li XK, Yuan CF, Hao YL, et al. Porous Titanium-6 Aluminum-4 Vanadium cage has better osseointegration and less micromotion than a poly-ether-ether-ketone cage in sheep vertebral fusion. Artif Organs 2013;37(12):E191–201.
83. Li X-K, Yuan C-F, Wang J-L, Zhang Y-Q, Zhang Z-Y, Guo Z. The treatment effect of porous titanium alloy rod on the early stage talar osteonecrosis of sheep. PLoS One 2013;8(3):e58459.
84. Kumar A, Nune K, Misra R. Biological functionality and mechanistic contribution of extracellular matrix-ornamented three dimensional Ti-6Al-4V mesh scaffolds. J Biomed Mater Res A 2016;104(11):2751–63.
85. Fielding G, Bose S. SiO_2 and ZnO dopants in three-dimensionally printed tricalcium phosphate bone tissue engineering scaffolds enhance osteogenesis and angiogenesis in vivo. Acta Biomater 2013;9(11):9137–48.
86. Mangano F, Macchi A, Shibli JA, Luongo G, Iezzi G, Piattelli A, et al. Maxillary ridge augmentation with custom-made CAD/CAM scaffolds. A 1-year prospective study on 10 patients. J Oral Implantol 2014;40(5):561–9.